applied sciences

MDPI

*Article*

# Image Enhancement Method in Underground Coal Mines Based on an Improved Particle Swarm Optimization Algorithm

**Lili Dai [1], Peng Qi [2], He Lu [1,2], Xinhua Liu [2,*], Dezheng Hua [2] and Xiaoqiang Guo [2]**

[1] Institute of Smart Materials and Applied Technology, Lianyungang Normal College, Lianyungang 222006, China
[2] School of Mechatronic Engineering, China University of Mining and Technology, Xuzhou 211006, China
* Correspondence: liuxinhua@cumt.edu.cn

**Abstract:** Due to the poor lighting conditions and the presence of a large amount of suspended dust in coal mines, obtained video has problems with uneven lighting and low differentiation of facial features. In order to address these problems, an improved image enhancement method is proposed. Firstly, the characteristics of underground coal mine images are analyzed, and median filtering is selected for noise removal. Then, the gamma function and fractional order operator are introduced, and an image enhancement algorithm based on particle swarm optimization is proposed. Finally, several experiments are conducted, and the results show that the proposed improved algorithm outperforms classical image enhancement algorithms, such as MSR, CLAHE and HF. Compared with the original image, the evaluation metrics of the enhanced Yale face images, including average local standard deviation, average gradient, information entropy and contrast, are improved by 113.1%, 63.8%, 22.8% and 24.1%, respectively. Moreover, the proposed algorithm achieves a superior enhancement effect in the simulated coal mine environment.

**Keywords:** image enhancement; particle swarm optimization; gamma transform; fractional order; coal mine environment



**Citation:** Dai, L.; Qi, P.; Lu, H.; Liu, X.; Hua, D.; Guo, X. Image Enhancement Method in Underground Coal Mines Based on an Improved Particle Swarm Optimization Algorithm. *Appl. Sci.* **2023**, *13*, 3254. https://doi.org/10.3390/app13053254

Academic Editor: Alessandro Chiolerio

Received: 21 January 2023
Revised: 21 February 2023
Accepted: 2 March 2023
Published: 3 March 2023



## 1. Introduction

With the rapid improvement of coal mine informationization [1–3], underground coal mine image enhancement has drawn considerable attention in image processing. However, due to the complicated underground environment and poor lighting conditions, coal mine image enhancement is a challenging problem. Usually caused by the presence of a large amount of suspended dust, the images obtained in coal mines are not clear and prone to the halo phenomenon [4,5]. This kind of image makes it difficult to identify the region of interest, which reduces the quality of the image and the visual effect of human eyes [6,7]. Therefore, it is necessary to enhance the image by image enhancement technology to highlight the detailed features of the original image and make the original blurred and low recognition image clear [8–10]. Image enhancement is essentially a noise reduction process, which enriches the favorable information in the image and eliminates or suppresses the worthless parts. At present, with the continuous innovation of image enhancement technology, many image enhancement algorithms have emerged [11–13], including gray transformation enhancement algorithms, frequency transformation enhancement algorithms and enhancement algorithms based on Retinex. However, the current image enhancement algorithms mainly focus on improving the brightness and contrast of uneven illumination images [14–16], while the problems of magnifying noise and losing weak texture detail information of mine images still exist.

The image enhancement methods based on gray transformation mainly improve the brightness and contrast of the image through histogram equalization. Liu et al. [17] optimized global histogram normalization and local histogram normalization through global and local constraints, which greatly improves the contrast of the original image. Based

on the dark primary color prior and the CLAHE algorithm, a novel image enhancement method was presented by Wu et al. [18] to get clear images in the foggy coal mine. Aiming to solve the problem of reading errors caused by color deviation under abnormal light sources, Niu et al. [19] proposed an adaptive color barcode image restoration algorithm. Considering that medical images acquired at insufficient lighting conditions suffer from low contrast issues, Saravanan et al. [20] proposed a fuzzy and spline-based histogram equalization to perform contrast enhancement with medical images. In order to improve the effect of image acquisition under the condition of low illumination, Zhang et al. [21] adopted a low-illumination image enhancement algorithm based on multi-feature fusion. However, it can be seen from these studies that most algorithms focus only on the overall contrast of the image and have limited ability to suppress noise.

Frequency domain image enhancement methods, such as Discrete Cosine Transform (DCT), Discrete Wavelet Transform (DWT) and Fast Fourier Transform (FFT), decompose the image into subbands of different frequencies or directions and then process each subband separately. Wan et al. [22] found that the fusion of multiple methods can effectively improve the effect of image enhancement and developed an image enhancement method based on DCT and DWT. Aiming to alleviate the image distortion caused by refraction and absorption of light depending on depth and color of water, Banerjee et al. [23] proposed an underwater image enhancement algorithm based on DCT, DWT and FFT. The basic content of Retinex theory is that the color of an object is determined by its ability to reflect light waves rather than by the intensity of the reflected light. Ji et al. [24] proposed a Retinex algorithm based on a guided filter, aiming to solve the problem that nighttime images have many dark spaces and shadows with low resolution. Priyanka et al. [25] combined principal component analysis with a multi-scale retinex-based adaptive filter to enhance low-light-level images. Based on camera response and weighted least squares strategies, a details enhancement approach was proposed by Rahman et al. [26] to enhance low-light images. In order to reduce the loss of detailed information during image enhancement in low light environments, Sun et al. [27] proposed an image enhancement algorithm based on improved multi-scale Retinex and artificial bee colony. However, over-enhancement may occur in areas of the image that have salient information, and the visual effect of enhanced coal mine images still needs to be improved.

Existing low-illumination image enhancement algorithms inevitably cause an enhanced image to be over- or under-enhanced images after enhancement, resulting in color distortion, so some measures are needed to correct the images. Liu et al. [28] proposed a simple but effective low-light image enhancement algorithm based on gamma function correction to address uneven brightness. Using a fractional-order mask and the fusion framework to enhance the low-light image, a novel fractional-order fusion model (FFM) is presented by Dai et al. [29] for low-light image enhancement, which extracts more invisible contents in dark areas. Aiming to increase the information content and enhance the details of an image, Kanmani et al. [30] presented an image contrast enhancement algorithm, which uses an adaptive gamma correction technique aided by particle swarm optimization. However, it is a challenge to effectively combine the advantages of the above image enhancement methods.

In this paper, a gamma transformation and fractional order image enhancement algorithm based on particle swarm optimization are proposed, which removes noise and enhances the texture information of low-light images. Firstly, by analyzing the characteristics of underground coal mine images, a median filter is selected for image denoising. Moreover, gamma transformation is introduced to correct images with unbalanced grayscale, and facial detail features are enhanced by the fractional order operator. Experimental results show that the image enhancement performance indexes processed by the proposed algorithm, such as average local standard deviation, average gradient, information entropy and contrast, are superior to those of other classical image enhancement algorithms. Lastly, the validity of the proposed algorithm is verified by an image enhancement test in the simulated coal mine environment.

The remainder of this paper is organized as follows. In Section 2, the proposed improved particle swarm optimization algorithm is presented. The comparison experiments of image enhancement algorithms are carried out, and the effectiveness of the proposed improved algorithm is verified in Section 3. In Section 4, a face recognition system is built, and an occluded face recognition experiment is carried out in the simulated coal mine environment. Conclusions and future works are summarized in Section 5.

## 2. The Proposed Method

### 2.1. Improved Particle Swarm Optimization Algorithm

Particle Swarm Optimization (PSO) [31] is an optimization algorithm based on the foraging movement of the flock, in which the birds closest to the food will share information with the group so that the flock can narrow the search range to achieve the optimal foraging. Each particle can be measured in terms of position and speed at every moment, and its particle position and velocity can be expressed as $x_t = (x_{t1}, x_{t2}, \ldots, x_{tm})$ and $v_t = (v_{t1}, v_{t2}, \ldots, v_{tn})$. The optimal value is searched for each particle iteration, and the fitness of each particle iteration result is evaluated. After each iteration, all the individuals are compared to get the optimal individual optimal value ($p_{best}$); the optimal individual value from the beginning of the iteration to the current iteration is called the global optimal value ($g_{best}$). The process of particle iteration is a process in which the individual optimal value constantly replaces the global optimal value. When $p_{best}$ reaches the current optimal value, $p_{best}$ will replace $g_{best}$. When $p_{best}$ is not the current optimal value, $p_{best}$ will be discarded. The particles iterate until the stop condition is reached, and each particle iteration is updated with the following formula:

$$v_{t(d+1)} = \omega \times v_{td} + c_1 r_1 (p_{td} - x_{td}) + c_2 r_2 (g_{td} - x_{td}) \quad (1)$$

$$x_{t(d+1)} = x_{td} + v_{t(d+1)} \quad (2)$$

where $d$ is the number of iterations, $v_{t(d+1)}$ and $x_{t(d+1)}$ are the velocity and position of the particle after updating, $\omega$ is the inertia weight, $c_1$ and $c_2$ are the learning factors and $r_1$ and $r_2$ are the uniform random numbers within the range [0, 1].

#### 2.1.1. Fitness Evaluation Function

The value of the evaluation function corresponding to each particle determines the next update direction of the particle, which is related to whether a better image enhancement effect can be achieved. The coal mine image has the characteristics of low contrast and blurred details, while image enhancement requires information enhancement, and the effect of image enhancement after particle iteration should meet some evaluation indexes. In this paper, information entropy, gradient and variance are selected to form the suitability evaluation function $f_{itness}$, and $f_{itness}$ is defined as:

$$f_{itnesss} = \lambda_1 S + \lambda_2 H + \lambda_3 D \quad (3)$$

where $S$ is the information entropy, $H$ is the average gradient, $D$ is the variance, $\lambda_1$, $\lambda_2$ and $\lambda_3$ are the weighting coefficient, and the value of $\lambda_1$, $\lambda_2$ and $\lambda_3$ are 0.3, 0.5 and 0.2, respectively.

Information entropy is a common index for image quality evaluation, which reflects the richness of image information. Generally speaking, images with high information entropy are more colorful and of better quality. The definition of information entropy is as follows:

$$S = -\sum_{i=0}^{255} p_i \log p_i \quad (4)$$

where $p_i$ is the proportion of pixels with grayscale values in the image.

The gradient is the index that can reflect the difference between pixels. When the gradient is large, there is a significant difference in grayscale at the edge of the image, and the image is sharper. For an image $f(i, j)$, the gradient is defined as:

$$\nabla f(i,j) = \sqrt{\left(\frac{\partial f}{\partial i}\right)^2 + \left(\frac{\partial f}{\partial j}\right)^2} \tag{5}$$

For an image of size $L = m \times n$, the average gradient is:

$$H = \frac{\sum_{i,j \in L} \nabla f(i,j)}{m \times n} \tag{6}$$

Variance $D$ reflects the degree of dispersion of the image pixel value from the mean value, and a large standard deviation represents a clear image edge. For an image $f(i, j)$, the mean and variance are recorded as $\mu$ and $\sigma^2$, respectively:

$$\mu = \frac{\sum_{i,j \in L} f(i,j)}{m \times n} \tag{7}$$

$$D = \sigma^2 = \frac{\sum_{i,j \in L} (f(i,j) - \mu)^2}{m \times n} \tag{8}$$

The calculation flowchart of the fitness evaluation function proposed in this paper is shown in Figure 1.

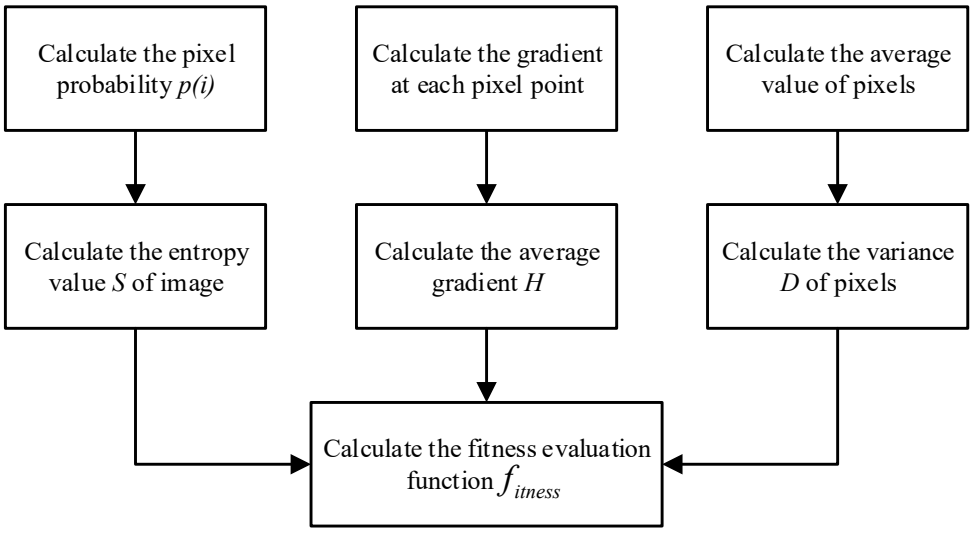


**Figure 1.** Flowchart of fitness evaluation function calculation.

#### 2.1.2. Inertia Weight and Learning Factor

The value of inertia weight $\omega$ will affect the searching ability of particles, and the range of values is usually [0.2, 1.2]. Inertia weight can be divided into fixed weight and dynamic weight, and the dynamic inertia weight factor will change with the number of iterations, which can maintain the search ability, and the particles with dynamic weight have higher exploration ability.

In the initial stage of the search, $\omega$ is generally set to be larger, and the particles have the ability to have a larger global search area. With the increase in the number of iterations, it is necessary to optimize the local search and then reduce the value of $\omega$. The common method is linear iterative decline:

$$\omega_t = \omega_{\max} - \frac{(\omega_{\max} - \omega_{\min})t}{t_{\max}} \tag{9}$$

where $\omega_t$ is the value of the first iteration, $\omega_{\max}$ and $\omega_{\min}$ are the maximum and minimum inertia weight, and the value of $\omega_{\max}$ and $\omega_{\min}$ are 0.8 and 0.2, respectively.

The learning factors $c_1$ and $c_2$ represent the weight of each particle, where $c_1$ is the private learning weight, and $c_2$ is the global social weight. The learning weight of the particle swarm is different at different stages in the process of optimization. When the value of $c_1$ is large, the particles have a trend around their own optimal. When the value of $c_2$ is large, the PSO is more like a global search method, and even more, it always tries to exploit new areas. In order to achieve a better optimization effect, this paper designs a way to define the learning factor, which varies with the number of iterations. At the beginning of the iteration, the value of $c_1$ is larger, and the particle swarm can explore more areas on its own. With the increase of the number of iterations, the value of $c_1$ becomes smaller, while the value of $c_2$ increases, and the particle swarm learns more from the social global optimal. Through the comparison of several local optimal solutions, the global optimal solution will be found. The learning factor update is as follows:

$$c_1 = c_{1a} - 0.01(c_{1a} - c_{1b})t \tag{10}$$

$$c_2 = c_{2a} - 0.01(c_{2b} - c_{2a})t \tag{11}$$

where $c_1$ and $c_2$ are the current learning factors, $c_{1a}$ and $c_{2a}$ are the initial value of the learning factors, $c_{1b}$ and $c_{2b}$ are the final values of the learning factor, $t$ is the current iteration and the value of $c_{1a}$, $c_{2a}$, $c_{1b}$ and $c_{2b}$ are set to 2.5, 2.5, 0.5 and 2.2, respectively.

### *2.2. Gamma Transform and Fractional Order Image Enhancement*

#### 2.2.1. Gamma Transform

Gamma transform [32] can effectively improve the illumination quality of an image and construct a gamma function for image correction. The definition of gamma transform of a 2-dimensional image is as follows:

$$G(i,j) = cI(x,y)^{\gamma} \tag{12}$$

where $I(x, y)$ is the input image, $G(x, y)$ is the output image, $c$ and $\gamma$ are the strength parameter, $c$ is the intensity range, $\gamma$ is the intensity factor, the value of $c$ is 1 in this paper and the effect of different $\gamma$ is shown in Figure 2.

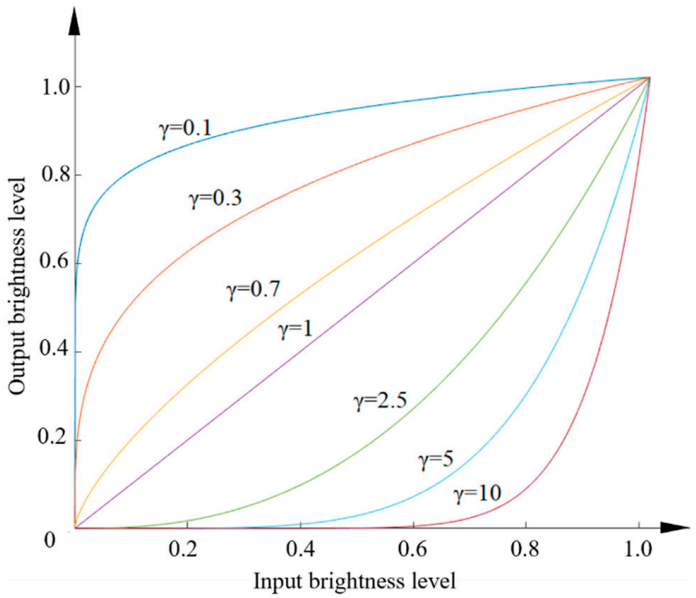


**Figure 2.** The gamma function curve with different values.

As can be seen from Figure 2, when the value of $\gamma$ is less than 1, the brightness of the output image is brighter than that of the input image, and the transformation has the effect of brightness enhancement. When the value of $\gamma$ is more than 1, the brightness of the output image is attenuated compared with the input image. When using gamma transform to realize image enhancement, it is generally desired to achieve a larger enhancement of luminance in the low-illuminance region and a small enhancement in the high-illuminance region. We randomly select a face in the Yale face dataset as the test image, and the enhancement effects of different $\gamma$ are shown in Figure 3 below.


**Figure 3.** Image enhancement effect with different gamma values.

2.2.2. Fractional Order Detail Enhancement

Three types of fractional order differentiation are commonly used, namely the Grünwald–Letnikov definition (G–L), the Riemann–Liouville definition (R–L) and the Caputo definition [33]. The Caputo definition is a modified form of G–L, which is given in a differential form and defined as follows:

$$ {}_aD_x^v f(x) = \frac{1}{\Gamma(m-v)} \int_a^x \frac{1}{(x-\xi)^{v-m+1}} f^{(m)}(\xi) d\xi \tag{13} $$

where $a$ and $x$ are the upper and lower limits of the integral, $v$ is the order of differentiation, $m$ is a positive integer that satisfies $m-1 < v < m$ and $\Gamma(v)$ is the gamma function.

When $m = 1$ and $a = 0$:

$$ {}_aD_x^v f(x) = \frac{1}{\Gamma(1-v)} \int_0^x \frac{1}{(x-\xi)^{v}} f'(\xi) d\xi \tag{14} $$

By dividing the interval $[0, x]$ into $N$ equal parts, the size of each part is $\Delta x = x/N$, and $f_0 = f(0), f_1 = f(x/N), \ldots, f_k = f(kx/N), \ldots, f_N = f(x)$. Then the approximate expression of Equation (14) can be obtained from the definition:

$$ {}_aD_x^v f(x) \approx \frac{1}{\Gamma(1-v)} \sum_{k=0}^{N-1} \int_0^x \frac{1}{(x-\xi)^{v}} f'(\xi) d\xi \tag{15} $$

According to the first-order derivative difference format:

$$ \begin{aligned} {}_aD_x^v f(x) \approx{}& \tfrac{F_N}{\Gamma(2-v)} + \tfrac{(2^{1-v}-2*1^{1-v}) f_{N-1}}{\Gamma(2-v)} + \ldots \\ &+ \tfrac{[(N-k+1)^{1-v}+(N-k-1)^{1-v}-2*(N-k)^{1-v}] f_{N-1}}{\Gamma(2-v)} \\ &+ \ldots + \tfrac{(N-1)^{1-v}-N^{1-v}}{\Gamma(2-v)} \end{aligned} \tag{16} $$

The first 3 coefficients on the right side of the equation are selected according to Equation (16):

$$ \begin{cases} a_0 = \frac{1}{\Gamma(2-v)} \\ a_1 = \frac{(2^{1-v}-2*1^{1-v})}{\Gamma(2-v)} \\ a_2 = \frac{[3^{1-v}-2*2^{1-v}+1]}{\Gamma(2-v)} \end{cases} \tag{17} $$

Fractional order differentiation is applied to adjacent pixels to fully exploit the image's local feature information and avoid over-smoothing of the enhanced image. This work uses a fractional order template of size $5 \times 5$ to perform the convolution operation and constructs fractional order operators in 8 directions as convolution kernels using the correlation coefficients of fractional order differentiation. The weight coefficients in the fractional order convolution kernel are related to the distance from its center pixel, and the specific fractional order operators are constructed, as shown in Figure 4 below. The inverse of the distance from the center pixel is used as the weight coefficient so that the pixels between the adjacent ones have a more significant influence on the weight.

| | | | | |
|---|---|---|---|---|
| $\frac{1}{\sqrt{8}}a_2$ | 0 | $\frac{1}{2}a_2$ | 0 | $\frac{1}{\sqrt{8}}a_2$ |
| 0 | $\frac{1}{\sqrt{2}}a_1$ | $a_1$ | $\frac{1}{\sqrt{2}}a_1$ | 0 |
| $\frac{1}{2}a_2$ | $a_1$ | $8a_0$ | $a_1$ | $\frac{1}{2}a_2$ |
| 0 | $\frac{1}{\sqrt{2}}a_1$ | $a_1$ | $\frac{1}{\sqrt{2}}a_1$ | 0 |
| $\frac{1}{\sqrt{8}}a_2$ | 0 | $\frac{1}{2}a_2$ | 0 | $\frac{1}{\sqrt{8}}a_2$ |

**Figure 4.** Fractional order weighted mask.

As shown in Figure 5, when the order of differentiation is an integer, the differentiation operation has the effect of gain for high-frequency signals, and its gain is non-linear with the growth of frequency and order. However, the high frequency will lead to ineffective noise suppression in the actual image enhancement. While fractional order differentiation is not as effective as integer order for high-frequency enhancement, fractional order differentiation can ensure that there is also a gain effect on the low-frequency part. Choosing the appropriate fractional order coefficients can achieve the enhancement of edge information while preserving the weak texture features of the background to a certain extent, which avoids making the image fall into over-enhancement. At present, the order of fractional differential enhancement is set manually. If the order is too small, it will lead to image sharpening. On the contrary, it will lead to the image detail enhancement is not obvious and cannot effectively suppress the noise. We randomly select a face in the Yale face dataset as the test image, and the enhancement effects of different $\nu$ are shown in Figure 6 below.

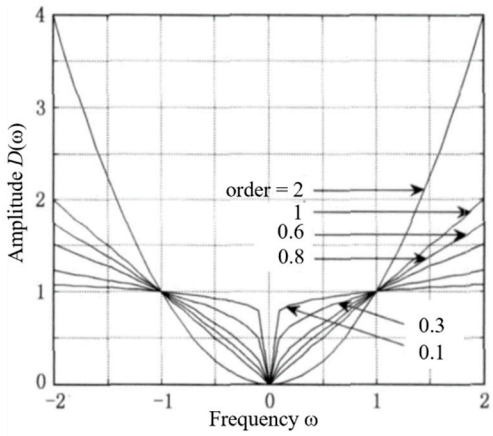


**Figure 5.** A-F character of fractional order.

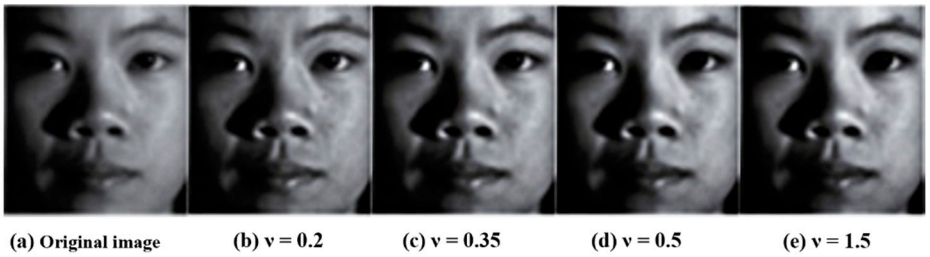


**Figure 6.** Image enhancement effect with different fractional orders.

### *2.3. Gamma Transform and Fractional-Order Image Enhancement Algorithm Based on Particle Swarm Seeking*

The specific process of the proposed improved algorithm is shown in Figure 7 below.

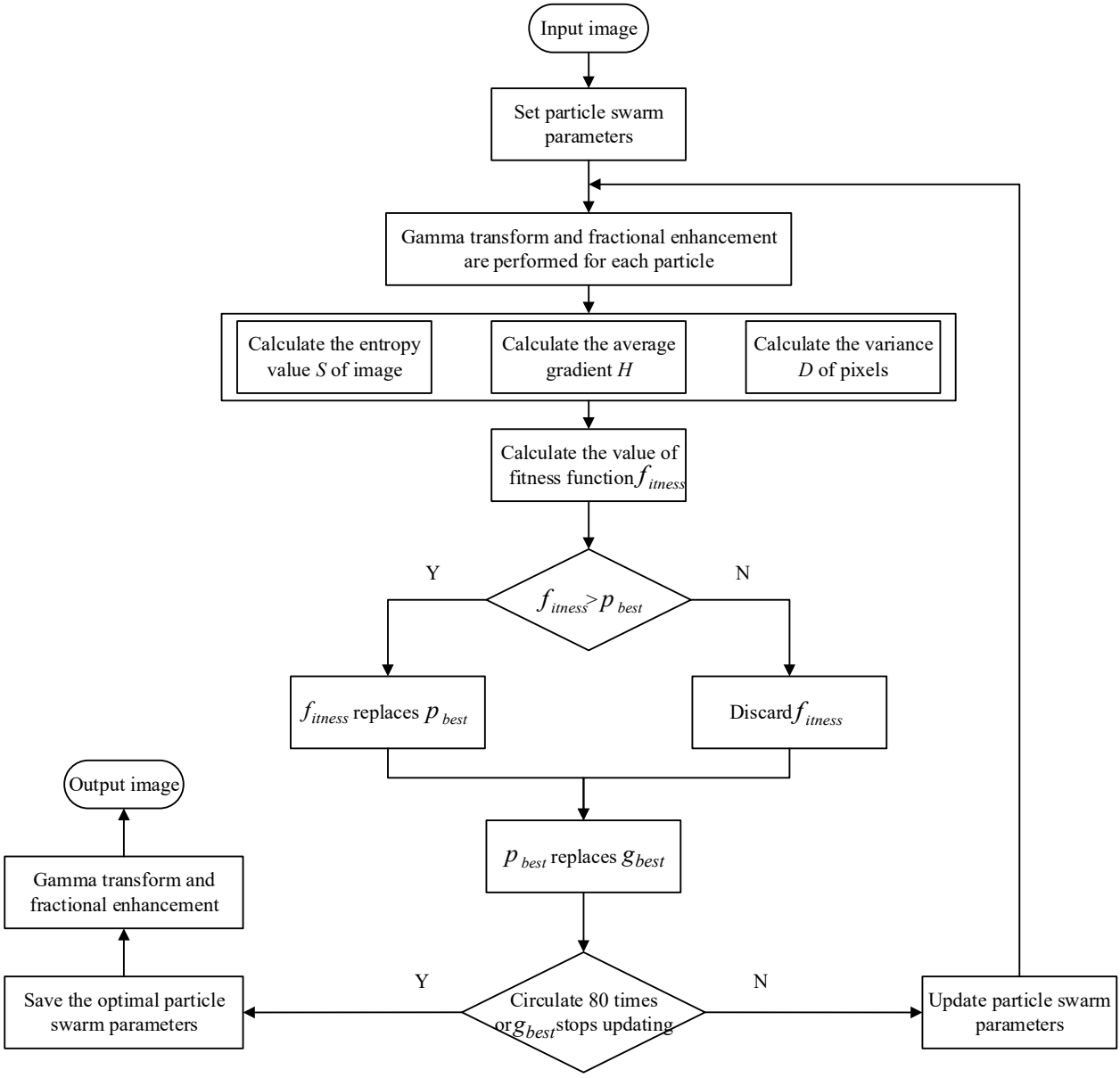


**Figure 7.** Flow chart of proposed image enhancement algorithm.

Step 1: Input the initial image;

Step 2: Set particle swarm parameters, mainly including the number of particles ($N = 300$), particle parameters $x_i$ and $v_i$, particle update parameters $\omega$, $c_{1a}$, $c_{2a}$, $c_{1b}$ and $c_{2b}$;

Step 3: Gamma transform and fractional order enhancement are performed on the input image, gamma parameters $\gamma \in (0, 3)$ and fractional order parameters $v \in (0, 1.5)$;

Step 4: Calculate the value of entropy $S$, the average gradient $H$ and the variance $D$ of the image, and calculate the value of $f_{itness}$ after each iteration;

Step 5: Compare $f_{itness}$ with $p_{best}$, and update $p_{best}$ if it is greater than $p_{best}$, otherwise discard it;

Step 6: If the condition is not satisfied, update the values of $c_1$, $c_2$, $x_i$ and $v_i$, and return to step 3; Otherwise, stop iteration;

Step 7: Using optimal gamma parameters and fractional order parameters $g_{best}(\gamma, v)$ for image enhancement.

## 3. Experimental Results and Analysis

### *3.1. Image Enhancement Comparison Experiment*

To verify the effectiveness of the proposed improved algorithm, the illumination inhomogeneous corridor image and the real image of an underground coal mine are selected for enhancement analysis experiments. Simulation experiments are conducted by MATLAB, and the proposed algorithms are compared with other classical image enhancement algorithms, including Multisim Scale Retinex (MSR), Contrast Limited Adaptive Histogram Equalization (CLAHE), Homomorphic Filter (HF) and the algorithm based on common PSO.

The image of the corridor with poor lighting conditions is selected for image analysis of different algorithms, and the image enhancement effects of each comparison algorithm and the proposed algorithm are shown in Figure 8 below.

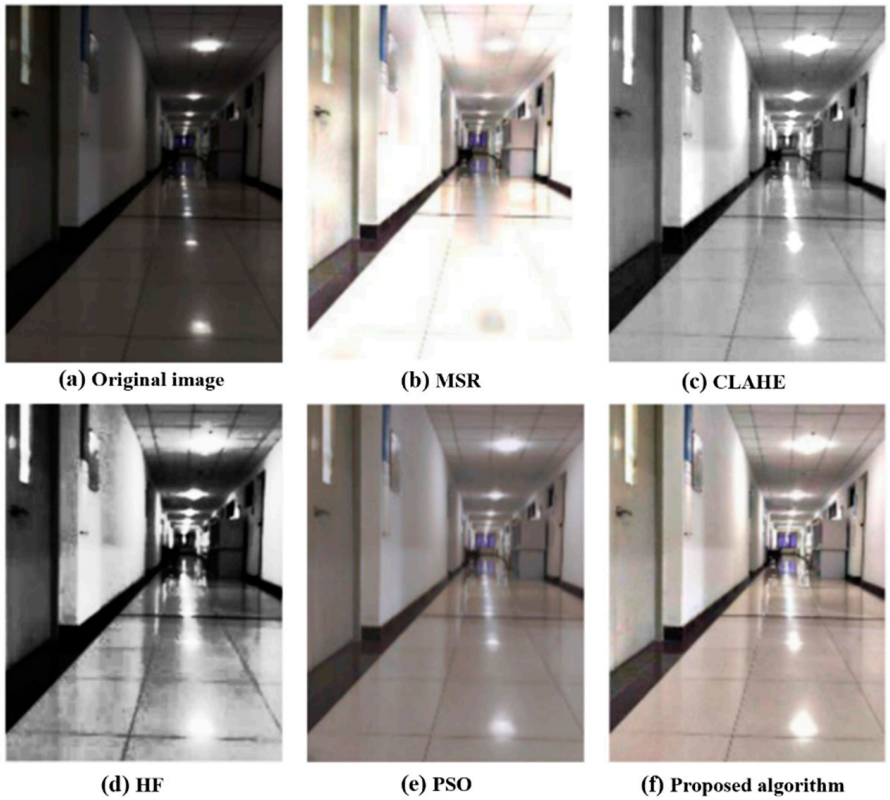


**Figure 8.** Comparison corridor image enhancement effect.

The image of the conveyor belt during coal mine production is selected for image analysis by different algorithms, and the image enhancement effects of each comparison algorithm and the proposed algorithm are shown in Figure 9 below.

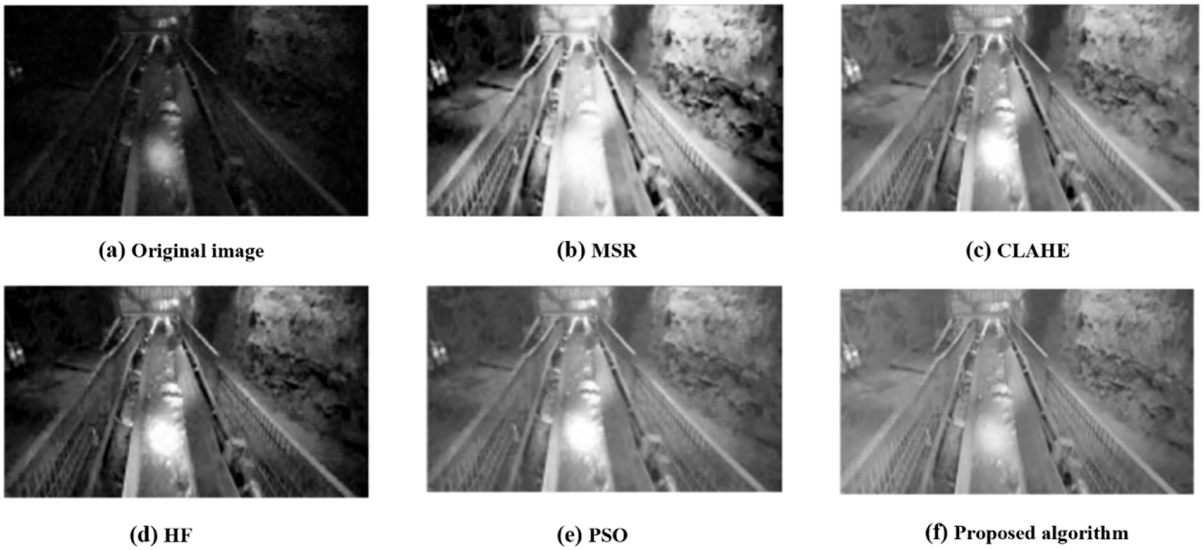


**Figure 9.** Comparison of mine video image enhancement effect.

The original images, Figures 8a and 9a, have low brightness resulting in insufficient image detail information. The contrast and brightness of images in Figures 8b and 9b are improved by processing with MSR, but the phenomenon of over-enhancement appears, and the brighter areas of the original images are not better suppressed. The overall brightness and sharpness of images in Figures 8c and 9c are improved after processing with CLAHE, but the phenomenon of halo appears in the brighter areas of the original images. The contrast of images Figures 8c and 9c is improved more after HF enhancement, but the overall brightness of the images is not improved enough compared with the original images, and some detailed information in the images is not reflected enough. After using the algorithm based on common PSO to process the images, the brightness and contrast of images in Figures 8e and 9e are better balanced, but the images still have detailed noise interference. The brightness of the image processed by the proposed algorithm is enhanced appropriately, and the original color and detail information of the image is retained better. Moreover, the noise is suppressed better while enhancing the image, which has a better visual effect compared with other image enhancement algorithms.

### *3.2. Analysis of Experimental Results*

The general evaluation metrics for image enhancement include Average Local Standard Deviation (ALSD), Average Gradient (AG), Information Entropy (IE) and Contrast.

In this paper, the above evaluation metrics are selected to evaluate images. The specific evaluation data are shown in Table 1 below, and the histogram of each enhancement algorithm after enhancement is shown in Figure 10.

**Table 1.** Comparison of corridor image enhancement algorithms.

| Metrics | Original Image | MSR | CLAHE | HF | PSO | Proposed Algorithm |
|---|---|---|---|---|---|---|
| ALSD | 25.85 | 31.24 | 44.24 | 55.94 | 38.52 | 73.47 |
| AG | 3.91 | 4.29 | 5.11 | 7.12 | 6.93 | 8.54 |
| IE | 6.27 | 6.72 | 6.69 | 7.15 | 6.79 | 7.23 |
| Contrast | 16,376.2 | 16,720.2 | 19,597.3 | 21,334.9 | 18,978.3 | 23,399.8 |

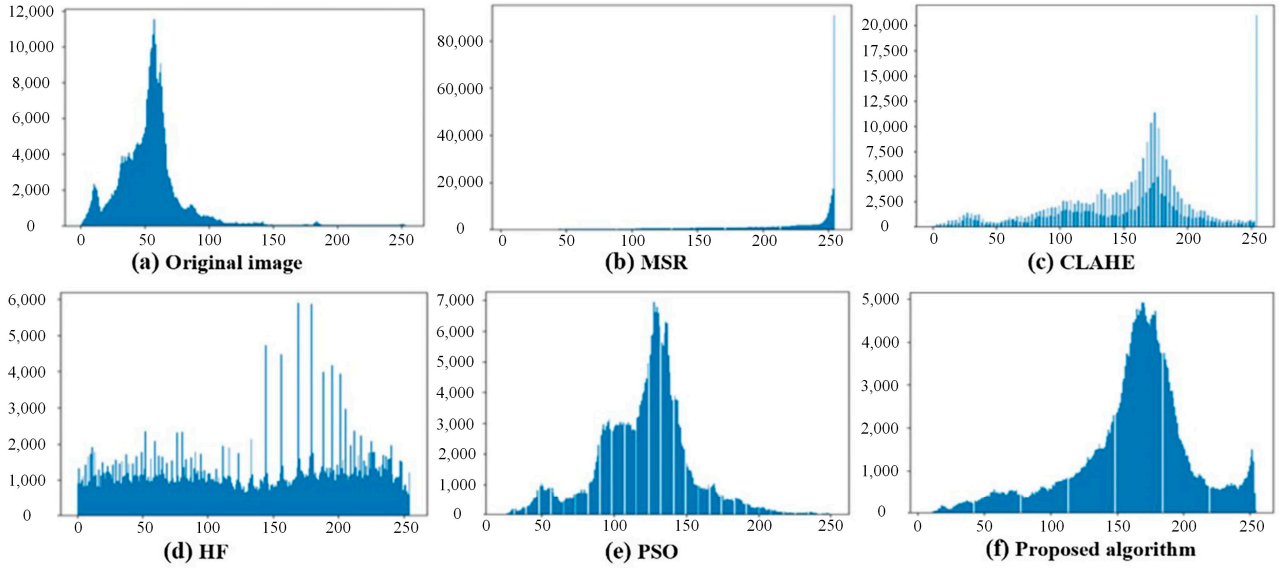


**Figure 10.** Enhancement histogram of corridor image.

Compared with the original image of the corridor, the enhanced images have been improved in terms of image brightness. However, the image after MSR enhancement appears over-enhanced, resulting in poor subjective image effects. The brightness of the image after CLAHE enhancement has been improved reasonably, but the visual effect is poor in terms of color retention. The image after HF enhancement has over-enhanced the contrast and neglected the detailed information, resulting in a lack of clarity in the detailed background. The algorithm based on common PSO has a good balance in all aspects, but the overall brightness and pattern details of the image still need to be improved compared with the proposed algorithm.

As shown in Figure 11 above, compared with the original image, ALSD, AG, IE and contrast of the image enhanced by the proposed algorithm improve by 184.2%, 118.4%, 15.3% and 42.8%, respectively, which are better than other algorithms. In terms of the enhanced histogram, the proposed algorithm takes into account the distribution of different pixel values of the image while enhancing the brightness and retaining more image detail information.

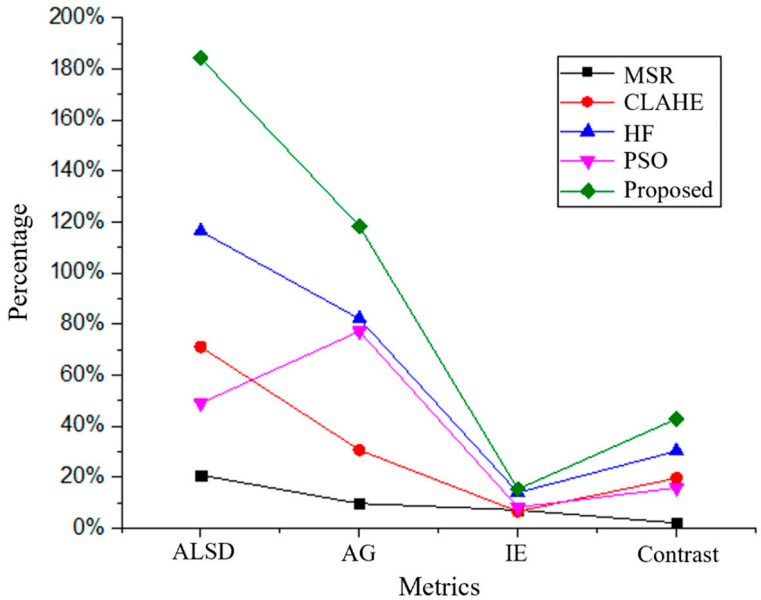


**Figure 11.** Percentage enhancement of corridor image.

For the analysis of the actual coal mine image, the image of the conveyor belt is selected, and the specific evaluation data are shown in Table 2 below. The histogram after enhancement by each enhancement algorithm is shown in Figure 12.

**Table 2.** Comparison of mine image enhancement algorithms.

| Metrics | Original Image | MSR | CLAHE | HF | PSO | Proposed Algorithm |
|---|---|---|---|---|---|---|
| ALSD | 29.62 | 35.43 | 39.66 | 42.15 | 39.89 | 44.71 |
| AG | 6.34 | 6.94 | 7.65 | 7.79 | 6.82 | 8.36 |
| IE | 6.11 | 7.38 | 7.26 | 7.42 | 7.14 | 7.96 |
| Contrast | 24,770.7 | 26,014.6 | 27,043.7 | 27,335.3 | 26,506.9 | 27,646.2 |

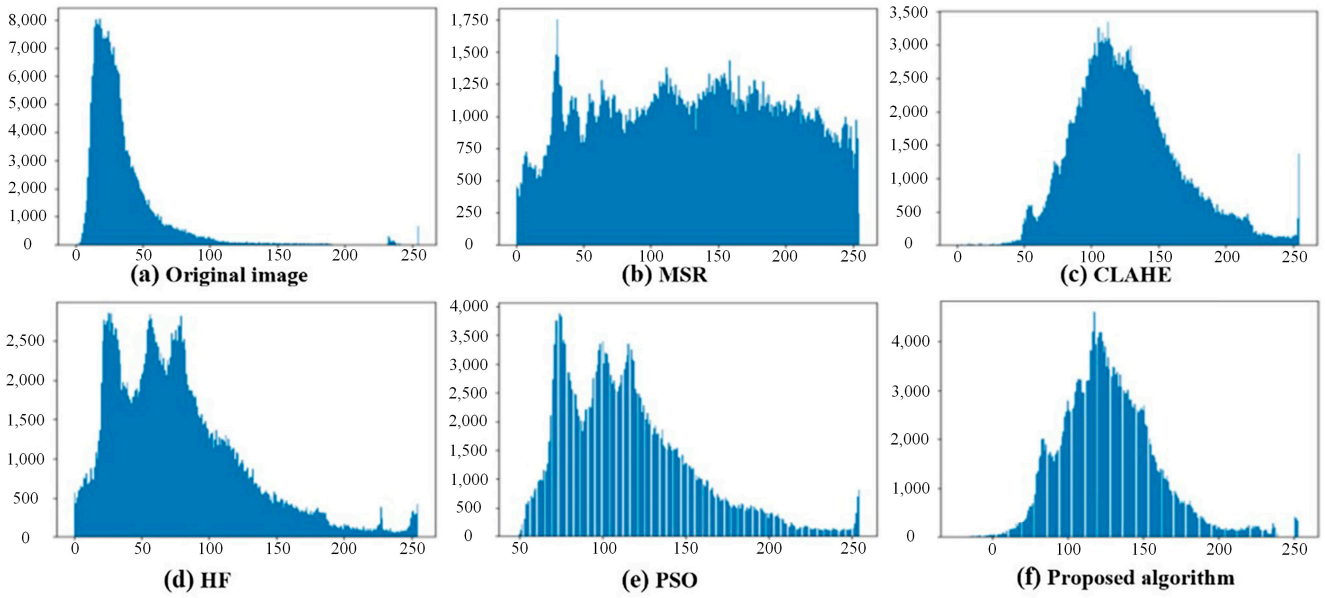


**Figure 12.** Enhancement histogram of mine image.

The actual coal mine image in Figure 9a has a darker background compared to the unevenly illuminated corridor image in Figure 8a. Subjectively, the images enhanced by each algorithm are enhanced in terms of image brightness. The brightness of the image enhanced by MSR is the most obvious, but there is over-enhancement in the belt brightness illumination region, which leads to the loss of belt edge contour information. The enhanced images after CLAHE and the algorithm based on common PSO show insignificant brightness enhancement in the regions with large brightness changes and still have noise interference. The image after HF enhancement focuses too much on the contrast between light and dark and loses the detailed information of the images.

As shown in Figure 13, compared with the original image, ALSD, AG, IE and contrast of the image enhanced by the proposed algorithm improve by 50.9%, 31.8%, 30.2% and 11.6%, respectively.

### *3.3. Test in Yale Dataset*

Through the above analysis, the proposed algorithm has good enhancement effects in both natural scenes and coal mines. To test the enhancement effect of the proposed algorithm for unevenly illuminated face images, face images subjected to different illumination conditions are selected from the extended Yale face dataset for testing experiments, and the images enhanced by the competitive algorithm are shown in Figure 14 below.

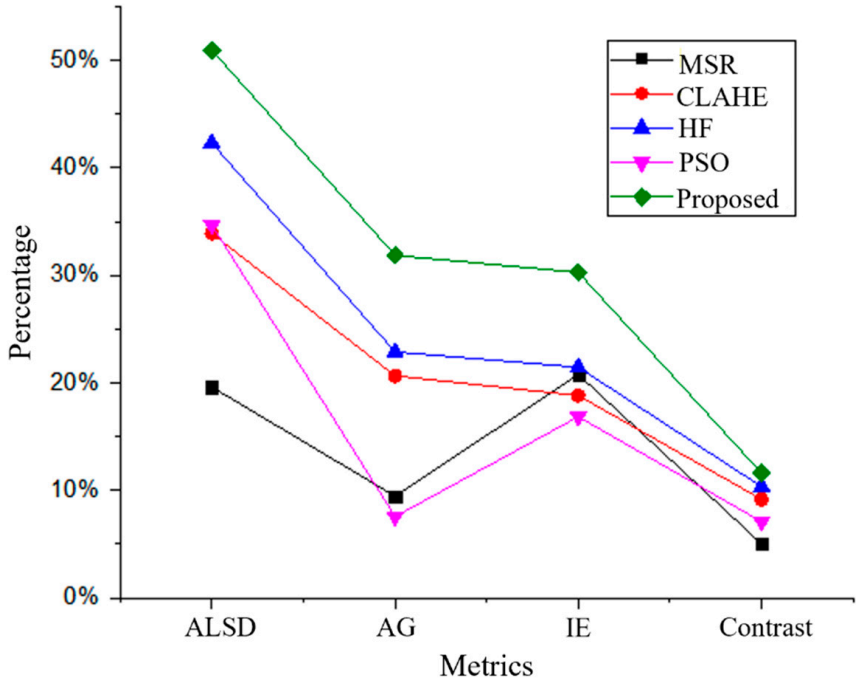


**Figure 13.** Percentage enhancement of mine image.

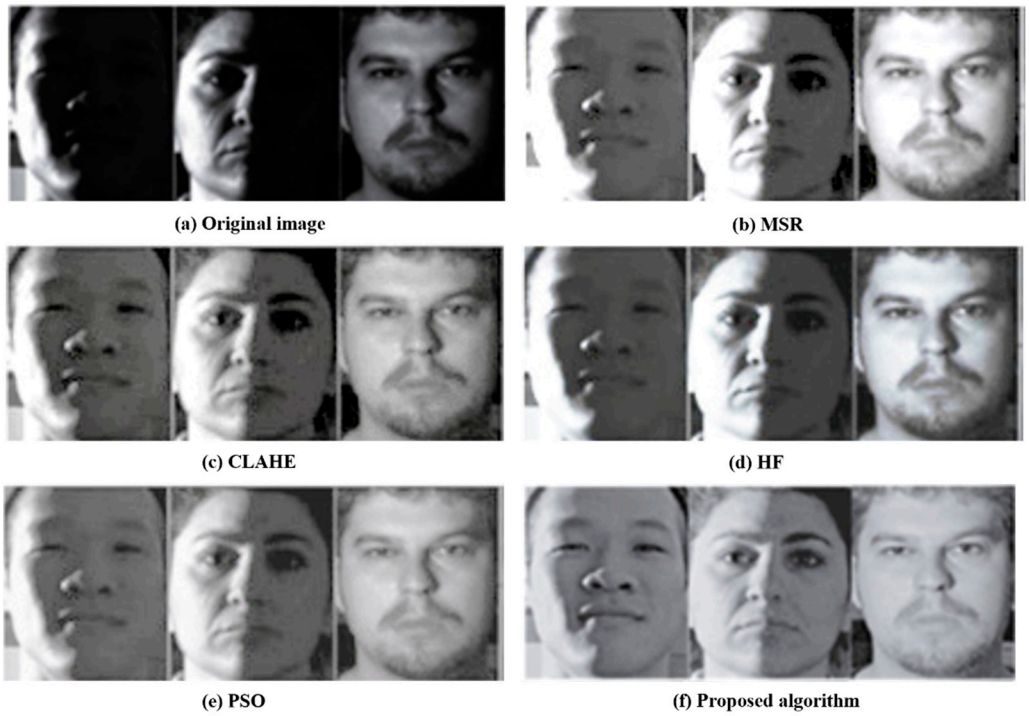


**Figure 14.** Comparison of the Yale face image enhancement effect.

As can be seen from the above image, compared with other images, the face image enhanced by the proposed algorithm has uniform brightness, clear face contour and rich detail features. For the analysis of the Yale face images, the specific evaluation data are shown in Table 3 below.

**Table 3.** Comparison of Yale face image enhancement algorithms.

| Metrics | Original Image | MSR | CLAHE | HF | PSO | Proposed Algorithm |
|---|---|---|---|---|---|---|
| ALSD | 27.74 | 33.34 | 41.95 | 49.05 | 39.21 | 59.09 |
| AG | 5.16 | 5.62 | 6.38 | 7.46 | 6.88 | 8.45 |
| IE | 6.19 | 7.05 | 6.98 | 6.97 | 6.91 | 7.60 |
| Contrast | 20,573.5 | 21,367.4 | 23,320.5 | 24,335.1 | 227,426 | 25,523.1 |

As shown in Table 3, compared with the original image, ALSD, AG, IE and contrast of the image enhanced by the proposed algorithm improve by 113.1%, 63.8%, 22.8% and 24.1%, respectively.

## 4. Application in Simulated Coal Mine Environment

The experiment in a simulated coal mine environment is used to verify the feasibility of the proposed image enhancement algorithm, and the part of facial images with coal ash is shown in Figure 15 below. The miner face dataset contains 840 images from 40 people, of which 756 are used as training sets, and the remaining 84 are used as test sets.


**Figure 15.** Part of facial images with coal ash.

The experiment is carried out in the underground garage of the School of Mechanical and Electrical Engineering. A surveillance camera is set up above the corner to obtain images, and an LED light source is selected to adjust the light intensity. The equipment involved in the experiment is shown in Figure 16 below.

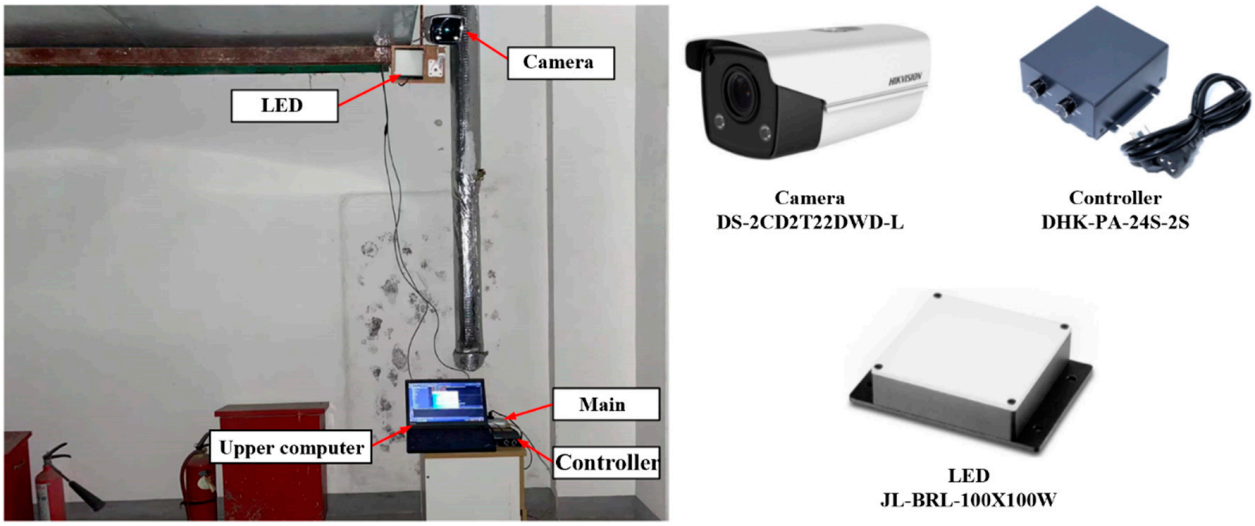


**Figure 16.** Experimental facilities.

After the experimental bench is built, the face image dataset is imported into the face recognition system, and a face recognition test is conducted. The recognition result column will output the number of recognized faces and the corresponding identity. The specific software interface is shown in Figure 17 below.

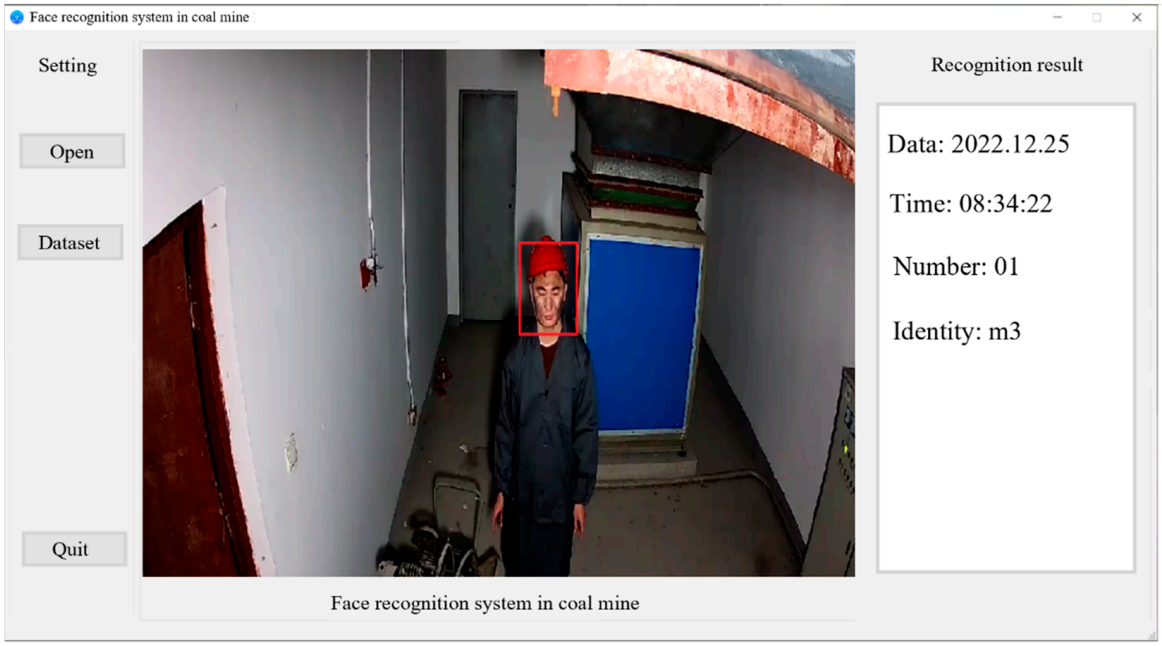


**Figure 17.** Experimental scene test.

The face recognition network, VGG-16, is trained on the original image dataset and the enhanced facial image dataset, respectively. The precision, recall and F1-score of the face recognition system are calculated, and the specific experimental results are shown in Table 4 below.

**Table 4.** Experimental results of face recognition.

| Dataset \ Metrics | Precision | Recall | F1-Score |
|---|---|---|---|
| Original image | 89.89% | 90.07% | 89.47% |
| Enhanced image | 92.44% | 93.44% | 92.44% |

As shown in Table 4, the evaluation indexes of the face recognition system, including accuracy, recall and F1-score, are improved by about 3% after the image enhancement. It can be proved that the proposed image enhancement algorithm is useful for improving the face recognition rate in underground coal mine environments.

## 5. Conclusions and Future Work

In this paper, a gamma transformation and fractional order image enhancement algorithm based on particle swarm optimization are proposed. By analyzing the characteristics of coal mine images, median filtering is selected for image denoising. The gamma function is introduced to correct images with too high or too low grayscale, and image detail features are enhanced by the fractional order operator. In addition, the proposed algorithm is applied to the face images with uneven lighting in the extended Yale face dataset, and the obtained enhanced images have a better visual effect, significant brightness enhancement and clearer face contour. Compared with the original image, the various evaluation indicators of the Yale face images enhanced by the proposed improved algorithm, including ALSD, AG, IE and contrast, are improved by 113.1%, 63.8%, 22.8% and 24.1%, respectively, which are better than other classical algorithms such as MSR, CLAHE and HF. Finally, this work conducts face recognition experiments in a simulated coal mine environment and achieves very superior experimental results.

This paper verifies the effectiveness of the proposed image enhancement algorithm for coal mine images. However, this work has only been carried out in a simulated coal mine environment, and no experimental validation has been carried out in an actual coal mine, and the next step is to carry out experiments in the working areas of a coal mine.

**Author Contributions:** Methodology, L.D.; Software, X.G.; Validation, P.Q. and D.H.; Formal analysis, X.L.; Investigation, H.L. All authors have read and agreed to the published version of the manuscript.

**Funding:** This research was funded by the National Natural Science Foundation of China (No. 51975568), the Independent Innovation Project of "Double-First Class" Construction of China University of Mining and Technology (2022ZZCX06), the Natural Science Foundation of Jiangsu Province under Grant (BK20191341), the Jiangsu Funding Program for Excellent Postdoctoral Talent (2022ZB519), the China Postdoctoral Science Foundation under Grant (2022M723387), Qing Lan project for excellent teaching team of Jiangsu province (2022) and Priority Academic Program Development of Jiangsu Higher Education Institutions (PAPD).

**Data Availability Statement:** The main data is presented in the text, and there is no new data.

**Conflicts of Interest:** The authors declare that there is no conflict of interest regarding the publication of this article.

## References

1. Wang, J.F.; Feng, L.J.; Zhao, Z.; Yu, H.J. Research on Underground Coal Mine Production Process Anlysis and Informatization. In Proceedings of the International Conference on Engineering Materials, Energy, Management and Control, Beijing, China, 22–23 January 2011; Volume 171–172, pp. 278–282. [CrossRef]
2. Zhong, T.; Lou, P.J.; Ruan, H.X.; Zhang, B. Construction of Coal Mine Comprehensive Informatization Based on Kilomega Fiber-optic Industry Ether Ring Network. In Proceedings of the International Conference on Computer-Aided Design, Manufacturing, Modeling and Simulation (CDMMS 2011), Hangzhou, China, 13–16 September 2011; Volume 88–89, p. 448. [CrossRef]
3. Yu, K.; Zhou, L.J.; Liu, P.P.; Chen, J.; Miao, D.J.; Wang, J.S. Research on a Risk Early Warning Mathematical Model Based on Data Mining in China's Coal Mine Management. *Mathematics* **2022**, *10*, 4028. [CrossRef]
4. Tian, J.; Yin, X.J. Adaptive image enhancement algorithm based on the model of surface roughness detection system. *Eurasip J. Image Video Process.* **2018**, *2018*, 103. [CrossRef]
5. Fan, X.S.; Min, L.; Li, J.L.; Guo, H.W.; Feng, L.P.; Xu, Z.Y. Dim and Small Target Detection Based on Spiral Gradient Optimization Estimation and High-Order Correlation Enhancement. *IEEE Access* **2022**, *10*, 14767–14778. [CrossRef]
6. Jiang, D.; Li, G.F.; Sun, Y.; Kong, J.Y.; Tao, B. Gesture recognition based on skeletonization algorithm and CNN with ASL database. *Multimed. Tools Appl.* **2019**, *78*, 29953–29970. [CrossRef]

7. Hu, J.B.; Sun, Y.; Li, G.F.; Jiang, G.Z.; Tao, B. Probability analysis for grasp planning facing the field of medical robotics. *Measurement* **2019**, *141*, 227–234. [CrossRef]
8. Cheng, Y.; Li, B. Image Segmentation Technology and Its Application in Digital Image Processing. In Proceedings of the 2021 IEEE Asia-Pacific Conference on Image Processing, Electronics and Computers (IPEC), Dalian, China, 14–16 April 2021.
9. Qi, Y.; Yang, Z.; Sun, W.; Lou, M.; Lian, J.; Zhao, W.; Deng, X. A Comprehensive Overview of Image Enhancement Techniques. *Arch. Comput. Methods Eng.* **2022**, *29*, 583–607. [CrossRef]
10. Sun, Y.; Tian, J.; Jiang, D.; Tao, B.; Liu, Y.; Yun, J.; Chen, D. Numerical simulation of thermal insulation and longevity performance in new lightweight ladle. *Concurr. Comput. Pract. Exp.* **2020**, *32*, e5830. [CrossRef]
11. Tian, C.W.; Fei, L.K.; Zheng, W.X.; Xu, Y.; Zuo, W.M.; Lin, C.W. Deep learning on image denoising: An overview. *Neural Netw.* **2020**, *131*, 251–275. [CrossRef]
12. Goyal, B.; Dogra, A.; Agrawal, S.; Sohi, B.S.; Sharma, A. Image denoising review: From classical to state-of-the-art approaches. *Inf. Fusion* **2020**, *55*, 220–244. [CrossRef]
13. Liu, J.; Malekzadeh, M.; Mirian, N.; Song, T.-A.; Liu, C.; Dutta, J. Artificial Intelligence-Based Image Enhancement in PET Imaging: Noise Reduction and Resolution Enhancement. *PET Clin.* **2021**, *16*, 553–576. [CrossRef]
14. Huang, S.C.; Cheng, F.C.; Chiu, Y.S. Efficient Contrast Enhancement Using Adaptive Gamma Correction With Weighting Distribution. *IEEE Trans. Image Process.* **2013**, *22*, 1032–1041. [CrossRef] [PubMed]
15. Zhou, Z.G.; Sang, N.; Hu, X.R. Global brightness and local contrast adaptive enhancement for low illumination color image. *Optik* **2014**, *125*, 1795–1799. [CrossRef]
16. Rahman, H.; Paul, G.C. Tripartite sub-image histogram equalization for slightly low contrast gray-tone image enhancement. *Pattern Recognit.* **2023**, *134*, 109043. [CrossRef]
17. Liu, C.W.; Sui, X.B.; Kuang, X.D.; Liu, Y.; Gu, G.H.; Chen, Q. Optimized Contrast Enhancement for Infrared Images Based on Global and Local Histogram Specification. *Remote Sens.* **2019**, *11*, 849. [CrossRef]
18. Wu, D.M.; Zhang, S.Q.; IEEE. Research on Image Enhancement Algorithm of Coal Mine Dust. In Proceedings of the 1st Annual International Conference on Sensor Networks and Signal Processing (SNSP), Xi'an, China, 28–31 October 2018; pp. 261–265. [CrossRef]
19. Niu, W.; He, J.; Liu, X.; Huang, L.; Zhao, X. An Adaptive Recovering Algorithm for The Color Bar Code Image Based on Gamma Transforms. *J. Phys. Conf. Ser.* **2021**, *1952*, 022029. [CrossRef]
20. Saravanan, S.; Karthigaivel, R. A fuzzy and spline based dynamic histogram equalization for contrast enhancement of brain images. *Int. J. Imaging Syst. Technol.* **2021**, *31*, 802–827. [CrossRef]
21. Zhang, X.; Sun, X.; Wang, T. Low-illumination image enhancement algorithm based on multi-feature fusion. In *IOP Conference Series: Materials Science and Engineering*; IOP Publishing: Bristol, UK, 2020; Volume 799, p. 012038. [CrossRef]
22. Mustafa, W.A.; Yazid, H.; Khairunizam, W.; Jamlos, M.A.; Zunaidi, I.; Razlan, Z.M.; Shahriman, A.B. Image Enhancement Based on Discrete Cosine Transforms (DCT) and Discrete Wavelet Transform (DWT): A Review. In *IOP Conference Series: Materials Science and Engineering*; IOP Publishing: Bristol, UK, 2019; Volume 557, p. 012027. [CrossRef]
23. Banerjee, A.; Shivakumara, P.; Pal, S.; Pal, U.; Liu, C.L. DCT-DWT-FFT Based Method for Text Detection in Underwater Images. In Proceedings of the 6th Asian Conference on Pattern Recognition (ACPR), Jeju Island, Republic of Korea, 9–12 November 2021; Volume 13189, pp. 218–233. [CrossRef]
24. Ji, W.; Qian, Z.J.; Xu, B.; Zhao, D.A. A nighttime image enhancement method based on Retinex and guided filter for object recognition of apple harvesting robot. *Int. J. Adv. Robot. Syst.* **2018**, *15*, 1729881417753871. [CrossRef]
25. Priyanka, S.A.; Wang, Y.K.; Huang, S.Y. Low-Light Image Enhancement by Principle Component Analysis. *IEEE Access* **2019**, *7*, 3082–3092. [CrossRef]
26. Rahman, Z.; Aamir, M.; Pu, Y.F.; Ullah, F.; Dai, Q. A Smart System for Low-Light Image Enhancement with Color Constancy and Detail Manipulation in Complex Light Environments. *Symmetry* **2018**, *10*, 718. [CrossRef]
27. Sun, Y.; Zhao, Z.; Jiang, D.; Tong, X.; Tao, B.; Jiang, G.; Kong, J.; Yun, J.; Liu, Y.; Liu, X.; et al. Low-Illumination Image Enhancement Algorithm Based on Improved Multi-Scale Retinex and ABC Algorithm Optimization. *Front. Bioeng. Biotechnol.* **2022**, *10*, 865820. [CrossRef]
28. Liu, S.X.; Long, W.; Li, Y.Y.; Cheng, H. Low-light image enhancement based on membership function and gamma correction. *Multimed. Tools Appl.* **2022**, *81*, 22087–22109. [CrossRef]
29. Zhang, H.F.; Su, W.; Yu, J.; Wang, Z.F. Identity-Expression Dual Branch Network for Facial Expression Recognition. *IEEE Trans. Cogn. Dev. Syst.* **2021**, *13*, 898–911. [CrossRef]
30. Kanmani, M.; Narsimhan, V. An image contrast enhancement algorithm for grayscale images using particle swarm optimization. *Multimed. Tools Appl.* **2018**, *77*, 23371–23387. [CrossRef]
31. Shi, Y.; Eberhart, R. A modified particle swarm optimizer. In Proceedings of the 1998 IEEE International Conference on Evolutionary Computation Proceedings. IEEE World Congress on Computational Intelligence (Cat. No.98TH8360), Anchorage, AK, USA, 4–9 May 1998; pp. 69–73. [CrossRef]

32. David, D.; IEEE. Low Illumination Image Enhancement Algorithm Using Iterative Recursive Filter And Visual Gamma Transformation Function. In Proceedings of the Fifth International Conference on Advances in Computing and Communications (ICACC), Kochi, India, 3–5 September 2015; pp. 408–411. [CrossRef]
33. Sawangtong, W.; Sawangtong, P. An analytical solution for the Caputo type generalized fractional evolution equation. *Alex. Eng. J.* **2022**, *61*, 5475–5483. [CrossRef]